AIAA-98-4563

CASSINI ORBIT DETERMINATION FROM LAUNCH TO THE FIRST VENUS FLYBY

Duane C. Roth*, Mark D. Guman*†, Rodica Ionasescu*, Anthony H. Taylor*

Jet Propulsion Laboratory
California Institute of Technology
Pasadena, California

Abstract

This paper describes the Cassini orbit determination effort from injection through the first Venus flyby. Emphasis is placed on orbit determination modeling and the resulting orbit solutions. Key solutions supporting trajectory correction maneuver designs are presented and compared against the Venus flyby trajectory reconstruction. The trajectory reconstruction is discussed in detail, as it is currently the best representation available of the Cassini flight path.

Introduction

The Cassini mission is designed to conduct science investigations of the planet Saturn and its satellites, rings, and magnetosphere. The Cassini spacecraft, consisting of both a Saturn orbiter and a Titan atmospheric probe, will be injected into orbit around Saturn on 1 July 2004. During the first orbit, the Huygens probe separates from the orbiter and descends through Titan's atmosphere. The orbiter continues with a four year tour of the Saturn system, with multiple close flybys of Titan and several flybys of selected icy satellites.

To travel from Earth to Saturn, Cassini is placed on an interplanetary trajectory that includes gravity assists from two Venus flybys, an Earth flyby, and a Jupiter flyby. Figure 1 is a diagram of this trajectory as seen from the north ecliptic pole. The subject of this paper concerns orbit determination from launch to the first Venus encounter, the bold portion of the Figure 1 trajectory path.

Orbit determination results were used to achieve several objectives, including maintenance of the actual trajectory to a predefined nominal trajectory, efficient use of propellant, spacecraft safety considerations, mission and science planning, and science data reduction. In particular, orbit determination performed between launch and the first Venus flyby allowed Cassini to be safely navigated past Venus, as the spacecraft flew only 284 km above the surface of the planet (104 km above an atmospheric level deemed potentially dangerous to the spacecraft).

The first leg of the Cassini mission was extremely successful as all orbit determination goals and requirements were met. Of the four planned trajectory correction maneuvers, only the first two were needed. The final Venus approach orbit solution delivery, with a data cutoff one month prior to closest approach, yielded a prediction of the location of Venus periapsis to within one kilometer of the reconstructed value. The time of periapsis was predicted to within 35 milliseconds.

In the following sections, information regarding Cassini orbit determination for the first seven months of the mission is presented. The spacecraft trajectory is characterized first, followed by a brief description of the impact of Cassini's flight attitude and thruster geometry on the spacecraft's orbital dynamics. Next, orbit determination filter inputs and setup are discussed. These include a description of tracking data and *a priori* models for estimated and considered parameters. Results from selected orbit solutions are presented and compared against the current best reconstructed trajectory. Finally, model refinements which shall be used to improve orbit determination knowledge for the second Venus flyby are summarized.

Trajectory Description

Cassini lift off occurred from Cape Canaveral Air Station aboard a Titan IVB/Centaur launch system at the opening of the launch window on 15 October

*Member of Technical Staff, Navigation and Flight Mechanics Section.

†Senior Member, AIAA.

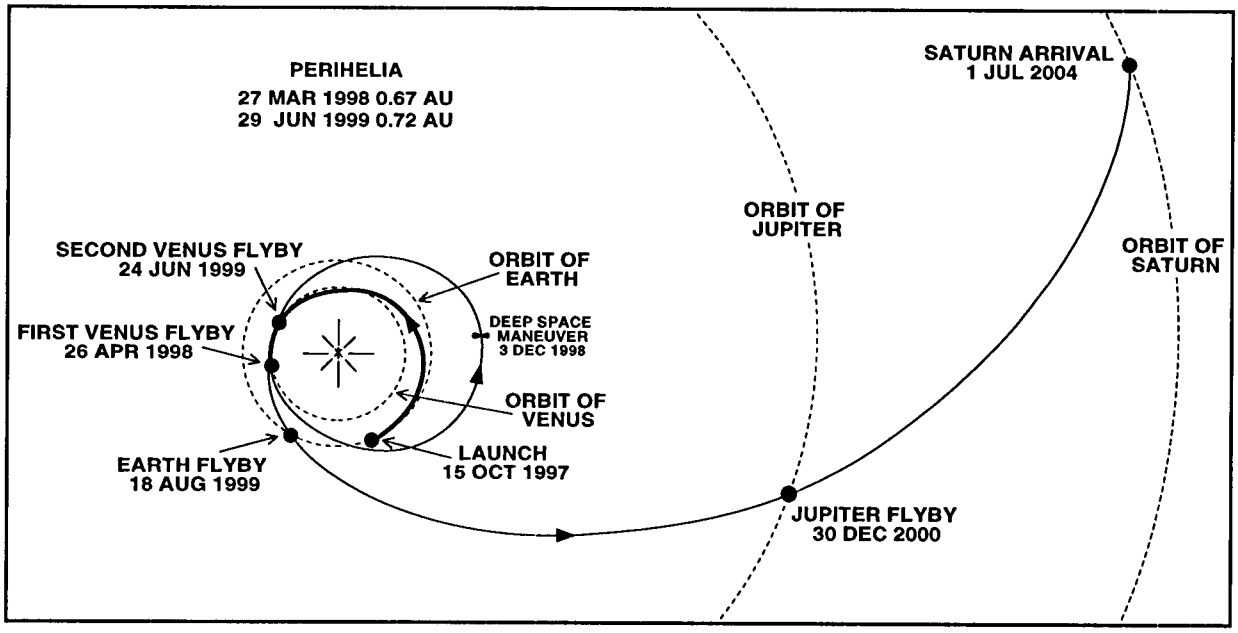

Figure 1. Cassini interplanetary trajectory.

1997. Approximately 40 minutes later, the spacecraft was successfully injected into a hyperbolic Earth escape trajectory. An estimate of the spacecraft state at injection was relayed from Lockheed Martin to the Jet Propulsion Laboratory and used as the starting point for the ensuing interplanetary orbit determination analysis.

Three trajectory correction maneuvers (TCMs) were planned to ensure Cassini's arrival to the targeted aimpoint at Venus on 26 April 1998. TCM1, designed to remove an injection bias and clean up injection errors, was executed on 9 November 1997. TCM2, designed to clean up orbit determination and execution errors from TCM1, was executed on 25 February 1998. TCM3, the last planned Venus approach maneuver (scheduled for 8 April 1998), was canceled. A fourth maneuver was planned after the Venus encounter to clean up orbit errors magnified by the flyby. TCM4, scheduled for 14 May 1998, was also canceled. Both TCM3 and TCM4 were canceled because they were not needed.[1]

Salient characteristics of the Cassini trajectory between injection and the first Venus flyby include the spacecraft geocentric declination (Figure 2) and heliocentric range (Figure 3). Excluding the day of launch, for the first 100 days the spacecraft declination was within 5 degrees of zero declination. Many previous papers have demonstrated the limitations of Doppler data at low declinations.[2,3] The spacecraft heliocentric range remained within 1.2% of 1 Astronomical Unit (AU) for the first 50 days after

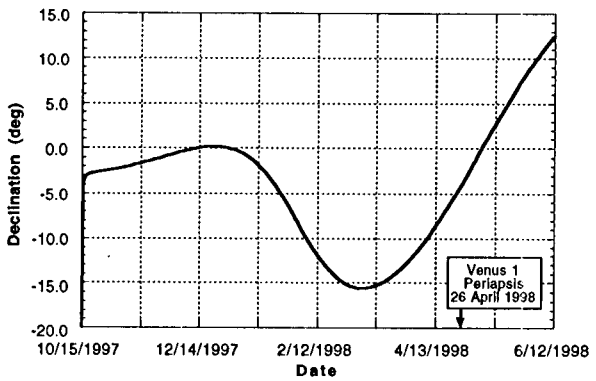

Figure 2. Geocentric declination.

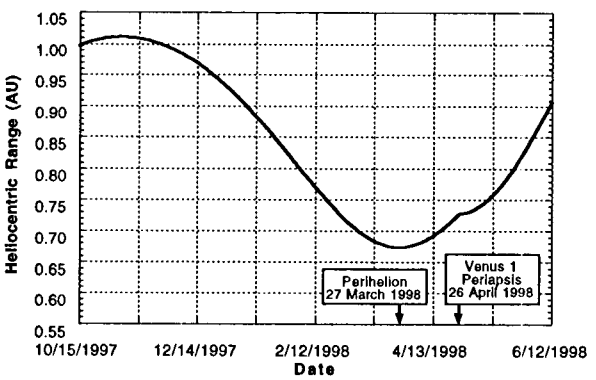

Figure 3. Heliocentric range.

launch. This characteristic is significant because solar pressure induced accelerations vary with the inverse square of heliocentric range. Since the range was nearly

constant, it was difficult to distinguish between the acceleration induced by the spacecraft radio-isotope thermoelectric generators (RTGs) and those induced by solar pressure.

Noteworthy events include an inferior solar conjunction on 9 February 1998 and passage through perihelion on 27 March 1998. The heliocentric range at perihelion was 0.67 AU.

Flight Attitude and Control

The Cassini spacecraft, shown in Figure 4, is three-axis stabilized. While within 2.7 AU of the Sun, the spacecraft -Z axis is nominally pointed at the Sun and the spacecraft -X axis is then pointed as close towards Earth as possible. In this attitude, the high gain antenna (HGA) shades and protects Cassini from adverse thermal conditions while communications are accomplished via one of the two omni-directional low gain antennae (LGA). Exceptions to this orientation exist for limited durations, most notably while executing maneuvers (attitude determined by maneuver requirements) and during a 25 day interval centered around solar opposition on 9 January 1999 (-Z axis is Earth pointed instead of Sun pointed).

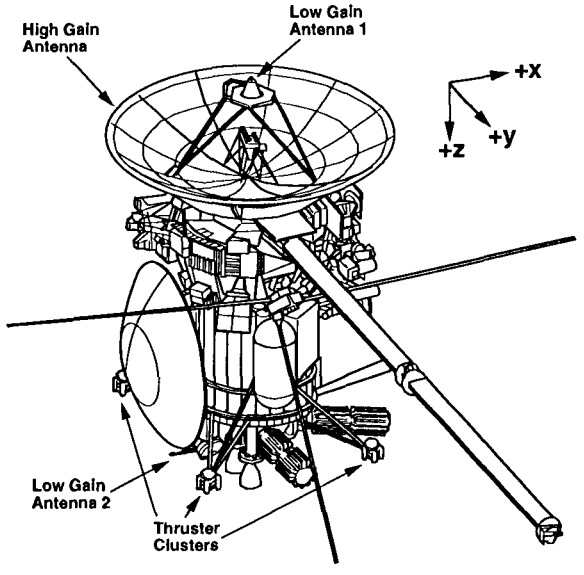

Figure 4. The Cassini spacecraft.

Cassini's flight attitude is controlled with the Reaction Control Subsystem (RCS), a set of 1 Newton monopropellant thrusters. The RCS is composed of four thruster clusters, each containing four thrusters. Two of the thrusters on each cluster are redundant. Figure 5, a simplified drawing of the plane containing these thrusters, shows the location and ΔV direction for each thruster. Roll attitude is controlled

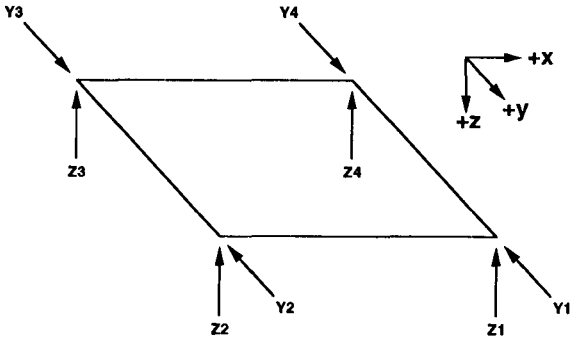

Figure 5. Thruster geometry.

with the coupled thrusters aligned parallel to the spacecraft Y axis (Y-thrusters). Pitch and yaw attitudes are controlled with the uncoupled thrusters aligned parallel to the spacecraft Z axis (Z-thrusters).

Because of thruster force mismatch and alignment offsets, maintaining roll attitude with the Y-thrusters will impart a net ΔV to the spacecraft. These ΔV's have not been observed however, because they are very small and currently in a direction nearly perpendicular to the ecliptic. This direction is the least well observed when using conventional Doppler and range tracking data types.

Because the Z-thrusters are uncoupled, maintaining pitch and yaw attitude imparts an observable ΔV to the spacecraft in the -Z direction. Since the -Z axis remains Sun pointed, visibility of this ΔV varies with the Earth-spacecraft-Sun (EPS) angle (Figure 6). The best visibility occurs near solar opposition (EPS=0°) and solar conjunction (EPS=180°) when the ΔV is directed along the line of sight. The worst visibility occurs when the EPS angle is around 90° and the ΔV is directed perpendicular to the line of sight.

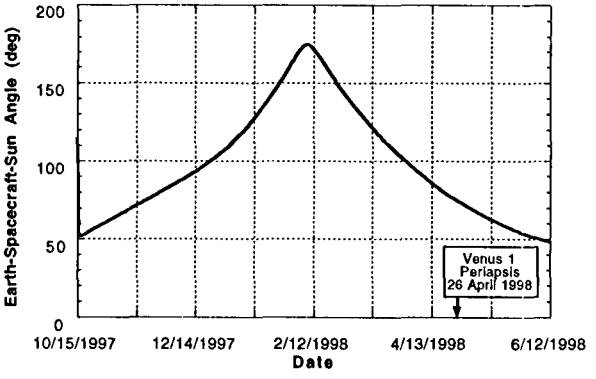

Figure 6. Earth-spacecraft-Sun angle.

The RCS is also used to execute small trajectory correction maneuvers. TCM2, which provided a ΔV of 0.2 m/s, was executed using the RCS. Cassini's main

engine, a redundant 445 N bipropellant system, is used to execute large maneuvers. TCM1, which provided a ΔV of 2.7 m/s, was executed using the main engine.

Tracking Data

Cassini is equipped with two low gain and one high gain antennae. Because the HGA was sun-pointed, only the two LGA's have been used to transpond tracking data so far. LGA 1 was used for the first ten days after launch and LGA 2 has been used since then. The HGA will be used during solar opposition and when the spacecraft heliocentric range exceeds 2.7 AU.

Tracking data was acquired by the Deep Space Network (DSN), with complexes in Spain, Australia, and the United States. X-band one-way Doppler, two-way Doppler and range, and three-way Doppler and range data types were collected. Two-way data, in which the uplink and downlink stations are the same, were the primary data types utilized for determining Cassini's orbit. One-way Doppler, in which the spacecraft generates the signal downlinked to Earth, and three-way data, in which the uplink and downlink stations are different, are more prone to systematic biases and therefore served primarily as sanity checks on the two-way data. Thirty-four meter aperture Beam Waveguide (BWG) and High-Efficiency (HEF) ground antennae acquired two-way tracking data. These antennae plus the 70 m aperture antennae acquired one-way and three-way data.

Doppler data was generally compressed to five minute intervals and was weighted between 0.2 and 1.0 mm/s (based on a one minute count time). Range data was acquired at intervals varying between 1 and 30 minutes, depending on the available signal strength, and was weighted between 5 m and 1 km. Troposphere and ionosphere calibrations were applied to all data.

Radiometric tracking data was scheduled continuously around launch and the Venus 1 encounter. Between these two events, tracking was scaled back to as little as one pass per week. Generally, coverage alternated between northern and southern hemisphere passes, enabling a better determination of spacecraft declination. Optical navigation data is not scheduled to begin until one year prior to Saturn orbit insertion.[4]

A Priori Models

Radiometric tracking data were combined with *a priori* models to refine estimates of several spacecraft dynamic parameters. In addition, certain systematic error sources were 'considered', i.e., some parameter errors were accounted for without actually estimating the parameters themselves. In this section, *a priori* models from the current best determined orbit are described and sensitivities to mismodeling are discussed. The current best determined orbit is a reconstruction of the Venus flyby and is based on a data arc extending from injection to 17 days after Venus closest approach. *A priori* models for earlier orbit solutions based on shorter data arcs may differ significantly since these models tend to evolve.

A priori models of estimated parameters include the spacecraft state, ΔV's, non-gravitational accelerations, Earth and Venus ephemerides, and the gravitational constant of Venus. *A priori* models of considered parameters include tracking station locations and media calibrations.

Spacecraft State

A priori values and uncertainties constraining the spacecraft state were initially based on the injection state and covariance supplied by Lockheed Martin. After a few weeks of tracking, these constraints were replaced with a diagonal covariance with essentially infinite variance, allowing orbit solutions to converge more quickly. By this time, the information content of the tracking data alone was sufficient to adequately determine the spacecraft state.

ΔV's

Several ΔV's were modeled and are listed in Table 1. TCM1 was modeled as a finite burn and 21 events were modeled as impulsive ΔV's. Seven impulsive ΔV's were modeled within the first two days after injection while Cassini was operating in the Center_Sun attitude control mode.[5] In this mode, the spacecraft attitude is propagated by gyros and is therefore susceptible to gyro drift errors. Attitude offsets of 3° to 4° were corrected with the RCS every several hours until an inertial attitude control mode was implemented using the star trackers. These attitude corrections imparted a ΔV of 3 - 5 mm/s directed primarily along the spacecraft -Z axis.

Small ΔV's of around 1 mm/s were observed during an attitude control computer reset and two Reaction Wheel Assembly (RWA) maintenance activities. Although the inertial attitude control mode was maintained before and after the attitude control computer reset, mode transitions occurred during the reset, prompting the RCS to respond. RWA maintenance activities, required periodically to lubricate the reaction wheel bearings, also caused the RCS to respond as the reaction wheels were spun up.

Seven ΔV's associated with TCM1 were estimated. Two days prior to executing the maneuver,

ΔV Event	Time (ET)	*A Priori* Value (mm/s)	*A Priori* Uncertainty (mm/s)
Center_Sun mode	15 Oct 1997 15:46	(0, 0, -4.0)	(0.5, 0.5, 2.0)
Center_Sun mode	16 Oct 1997 01:18	(0, 0, -4.0)	(0.5, 0.5, 2.0)
Center_Sun mode	16 Oct 1997 07:14	(0, 0, -4.0)	(0.5, 0.5, 2.0)
Center_Sun mode	16 Oct 1997 14:36	(0, 0, -4.0)	(0.5, 0.5, 2.0)
Center_Sun mode	16 Oct 1997 22:07	(0, 0, -4.0)	(0.5, 0.5, 2.0)
Center_Sun mode	17 Oct 1997 02:39	(0, 0, -4.0)	(0.5, 0.5, 2.0)
Center_Sun mode	17 Oct 1997 09:00	(0, 0, -4.0)	(0.5, 0.5, 2.0)
Attitude control computer reset	30 Oct 1997 19:25	(0, 0, 0)	(2.0, 2.0, 2.0)
Vent/prime main engines	8 Nov 1997 00:41	(0, 0, 0)	(0.5, 0.5, 2.0)
Tighten attitude control deadbands	9 Nov 1997 19:33	(0, 0, 0)	(0.5, 0.5, 2.0)
TCM1 roll wind turn	9 Nov 1997 19:44	(0, 0, 0)	(0.5, 0.5, 0.5)
TCM1 yaw wind turn	9 Nov 1997 19:53	(-2.6, -8.9, 0.2)*	(2.0, 2.0, 2.0)
TCM1	9 Nov 1997 20:01	finite burn model	finite burn model†
TCM1 yaw unwind turn	9 Nov 1997 21:08	(-2.6, -8.9, 0.2)*	(2.0, 2.0, 2.0)
TCM1 roll unwind turn	9 Nov 1997 21:17	(0, 0, 0)	(0.5 , 0.5, 0.5)
RWA maintenance	15 Jan 1998 04:52	(0, 0, -1.1)	(0.5 , 0.5, 0.5)
TCM2 turns and burn	25 Feb 1998 20:06	(-159.1, 45.5, 82.9)*	(4.5, 3.7, 3.9)*†
RCS firing, undetermined cause	17 Mar 1998 05:00	(0, 0, 0)	(0.5 , 0.5, 0.5)
RCS firing, undetermined cause	20 Mar 1998 00:00	(0, 0, 0)	(0.5 , 0.5, 0.5)
RCS firing, undetermined cause	21 Mar 1998 18:00	(0, 0, 0)	(0.5 , 0.5, 0.5)
Spacecraft safing	24 Mar 1998 19:12	(-0.1, 0, -5.0)	(0.3, 0.7, 1.0)
RWA maintenance	1 May 1998 16:00	(0, 0, -1.1)	(0.5, 0.5, 0.5)

* ΔV in Earth Mean Equator of 2000 coordinates. † *A priori* covariance is correlated. Only diagonal terms are given.

Table 1. A priori ΔV models along spacecraft-fixed axes except where noted.

the main engines were vented and primed. A half hour prior to TCM1, the attitude control deadbands were tightened and a roll and yaw turn were commanded to orient the spacecraft to the maneuver attitude. Following TCM1 execution on the main engine, yaw and roll turns were commanded to orient the spacecraft back to its nominal attitude. TCM1 pointing and ΔV magnitude were estimated instead of the three velocity components. *A priori* models for TCM1 included 279.8±1.0° right ascension, 24.3±0.9° declination, and 2.746±0.031 m/s ΔV magnitude. These nominal values are based on the TCM1 design. Implemented values differ by a small amount due to discretization of the commanded parameters. Right ascension and declination are specified in Earth Mean Equator of 2000 coordinates.

TCM2, with a ΔV an order of magnitude smaller than TCM1, was estimated as an impulsive maneuver. Tracking data was not acquired between the start of the yaw wind turn and the end of roll unwind turn because the tracking station lost lock with the spacecraft.[6] Because of this, the roll and yaw wind and unwind turns were not estimated separately. They were combined with the estimate of TCM2.

Four additional ΔV events were estimated. One was due to RCS thruster firing associated with spacecraft safing. The causes of three other very small ΔV's are currently not well understood. One theory attributes these ΔV's to RCS thruster firing to counter torques induced by thermal gradients in the propellant. The ΔV's occurred around one week prior to perihelion when no dynamic activities were scheduled. ΔV signatures were seen first in the Doppler data and partly confirmed later with RCS thruster on-time telemetry.

Non-gravitational Accelerations

Three accelerations spanning the entire data arc and several others spanning only a few days were estimated. Accelerations induced by solar pressure, asymmetric radio-isotope thermoelectric generator radiation forces, and spacecraft outgassing span the entire data arc. Unexpected short duration accelerations have also been observed after several of the thrusting events listed in Table 1. Because of sparse tracking data coverage, short duration accelerations were not discovered until after execution of TCM2, when three continuous tracking passes were scheduled immediately after TCM2 and one pass per day was scheduled for the next several days. Upon closer examination of earlier thrusting events, similar behavior was observed and modeled.

The largest of the estimated accelerations is due to solar pressure force. Solar pressure induced

accelerations vary with the inverse square of heliocentric range and may be separated into two parts. First, there is a direct effect accelerating the spacecraft away from the sun. At perihelion, the direct nominal acceleration is 37×10^{-12} km/s^2. Second, there is an indirect effect caused by the RCS' response to spacecraft torques induced by solar pressure. Z-thrusters will fire to counter torques and, because the spacecraft is Sun-pointed, will accelerate the spacecraft *towards* the sun. The indirect effect is roughly 15% of the direct effect, but radiometric data alone is not sufficient to distinguish between the two accelerations. Telemetry data indicating the frequency and duration of Z-thruster firings must also be analyzed. Because these two effects are not separable with radiometric data, telemetry data has been analyzed to corroborate the torque model, and only direct solar pressure accelerations are estimated. An *a priori* uncertainty of 3.5% of the nominal, direct value constrains the estimates of these accelerations. Solar pressure 'effective areas' are estimated, a synthesis of the actual sunlit areas and reflectivity coefficients, and are relative to a heliocentric range of 1 AU. Their nominal values and uncertainties are (0.00, 0.04, 20.92)±(0.72, 0.72, 0.72) m^2.

Another acceleration spanning the entire data arc is due to asymmetric radiation forces from the spacecraft RTGs. Three RTGs are located in a plane perpendicular to the Z axis near the base of the spacecraft. Radiation from these RTGs is emitted in all directions but is partially reflected back by the high gain antenna and shielding. This reflectance has the effect of accelerating the spacecraft in the -Z direction, or towards the Sun. Because the RTG power degrades with a time constant of over 100 years, this force is constant for all practical purposes. A secondary effect of these forces is a spacecraft torque which is countered with the Z-thrusters. *A priori* models of (-0.933, -0.107, -7.52)$\times 10^{-12}$ km/s^2 with 50% uncertainties have been derived from Reference 7.

A third acceleration spanning the entire data arc is due to spacecraft outgassing. Because it is modeled as an exponentially decreasing acceleration with an estimated time constant of nearly 29 days, the acceleration magnitude becomes insignificant a few months after injection. *A priori* models of (0, 0, 0)$\pm 10^{-11}$ km/s^2 are used to estimate the initial value of the acceleration. The time constant is also estimated with a 46±13 day *a priori* model.

Several short duration accelerations have also been estimated. These acceleration models extend for at most a few days and are caused by Z-thruster firings above the level required to control spacecraft torques induced by solar pressure and the RTG's. Short term accelerations associated with both RWA maintenance activities, the spacecraft roll near solar conjunction (to maintain LGA2 pointing towards Earth), TCM2, spacecraft safing, and spacecraft gravity gradients during the Venus flyby have been modeled. All short duration accelerations are modeled with *a priori* values of (0,0,0) km/s^2. For gravity gradient acceleration modeling on the incoming and outgoing asymptotes, the *a priori* uncertainties are 10^{-10} and 10^{-9} km/s^2 respectively. Time constants of 45 minutes (incoming) and 240 minutes (outgoing) are modeled. All other short duration accelerations are modeled with *a priori* uncertainties of 5×10^{-10} km/s^2 and 5 day time constants.

Other *A Priori* Models

To adequately fit the tracking data acquired during the Venus flyby, Earth and Venus ephemerides and the gravitational constant of Venus were estimated. *A priori* ephemeris values are from planetary ephemeris DE-403. As recommended by the developer of planetary ephemeris DE-403, *a priori* ephemeris uncertainties are from DE-405.[8] The gravitational constant of Venus was modeled as 324858.60±0.05 km^3/s^2. Prior to the Venus flyby, these error sources were considered, i.e., accounted for without being estimated.

Tracking station locations and media calibrations were considered. Station locations are from Reference 9, except Deep Space Stations (DSS) 34 and 54, which have since been modified to include the results of recent surveys. *A priori* station location uncertainties of 0.5 m are modeled. Media calibrations are provided by the Tracking System and Analytic Calibration group at JPL. *A priori* uncertainties for dry and wet troposphere calibrations are 1 and 4 cm respectively. *A priori* uncertainties for night and day ionosphere calibrations are 1 and 5 cm respectively.

Sensitivities to Mismodeling

The X-band tracking data acquired from Cassini provided visibility of ΔV's to within 0.02 - 0.03 mm/s in the line-of-sight direction. The excellent quality of this data resulted in greater insight of dynamic spacecraft activities but also caused the orbit determination filter to be extremely sensitive to mismodeling errors. Figure 7 conveys this sensitivity by displaying orbit determination results from two cases. For each case, a plot displays the orbit determination filter's estimate of B•R mapped to Venus closest approach for several data cutoffs around TCM2 (an appendix describing the B-plane coordinate system is attached). Formal one sigma error bars are included around each estimate. The most accurate estimate of B•R, based on the trajectory reconstruction,

Identifier	Purpose	Data Arc Start (GMT)	Data Arc End (GMT)
LP2D	TCM-1 preliminary design	15 Oct 1997 10:15	16 Oct 1997 22:59
LP15D	TCM-1 final design	15 Oct 1997 10:15	30 Oct 1997 06:57
LP47D	TCM-1 reconstruction	15 Oct 1997 10:15	27 Nov 1997 22:51
V1M88D	TCM-2 preliminary design	15 Oct 1997 10:15	26 Jan 1998 00:48
V1M69D	TCM-2 final design	10 Dec 1997 23:50	16 Feb 1998 02:55
V1M40D	TCM-3 preliminary design	15 Oct 1997 10:15	16 Mar 1998 06:56
V1M31D	TCM-3 final design	15 Oct 1997 10:15	26 Mar 1998 13:53
V1M25D	TCM-2 reconstruction	15 Oct 1997 10:15	29 Mar 1998 20:46
Reconstruction	Venus flyby reconstruction	15 Oct 1997 10:15	13 May 1998 20:26

Table 2. Summary of selected orbit solutions.

is superimposed over each plot. In the first case, short duration accelerations are not modeled. B•R estimates deviate several sigma from the reconstructed value and do not reconverge until data is acquired through the Venus flyby. The deviation is most pronounced around TCM2, because the post-TCM2 acceleration mismodeling corrupts the estimate of the TCM2 ΔV. In the second case, short duration accelerations are modeled. B•R estimates remain consistent with the reconstructed value over the entire plotted interval.

In both cases, Doppler data was weighted at 0.2 mm/s. Sensitivity to mismodeling errors can be mitigated by de-weighting the data, but also has the effect of increasing orbit uncertainties.

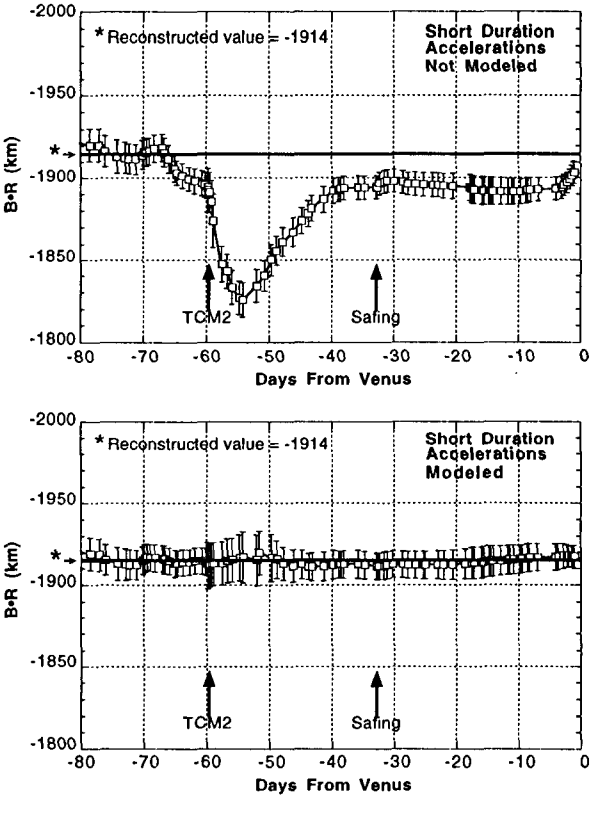

Figure 7. Orbit determination sensitivity to acceleration mismodeling.

Orbit Determination Results

Many orbit determination solutions were generated and analyzed between injection and the present. Sensitivities to various combinations of data types, data weights, data arc lengths, *a priori* values and uncertainties, and other factors were analyzed. Orbit determination results discussed in this section represent only those solutions used to reconstruct TCM1 and TCM2, design TCM1, TCM2, and TCM3, and precisely reconstruct the spacecraft trajectory from injection through the Venus flyby. Table 2 lists the names, purposes, and tracking data arc lengths of these orbit determination solutions. The naming convention refers to when orbit determination products became available. For instance, LP2D specifies product availability at **L**aunch **P**lus **2** **D**ays, V1M88D at **V**enus **1** **M**inus **88** **D**ays.

The solutions presented provide a history of the best orbit determination knowledge available at selected times. In addition, orbit determination performance is reviewed by removing maneuver execution errors from orbit estimates, mapping solutions to the Venus B-plane at closest approach, and then comparing the results. Finally, parameter estimates from the trajectory reconstruction are tabulated and discussed.

TCM Reconstruction

In an effort to determine and calibrate thruster performance, trajectory correction maneuvers are commonly reconstructed. Both TCM1, a main engine burn executed on 9 November 1997, and TCM2, an RCS burn executed on 25 February 1998 have been reconstructed.

The TCM1 reconstruction, identified as LP47D, was based on a data arc extending 18 days past the burn execution. Several additional ΔV events occurring within two days of TCM1 were estimated separately.

These ΔV's limit the reconstruction accuracy of TCM1 because the tracking data acquired between them is insufficient to determine velocity components perpendicular to the line of sight. These velocity components are therefore highly correlated, causing the estimate of them to be very dependent on *a priori* models.

TCM1 pointing and ΔV magnitude were estimated and are presented in Table 3 along with the nominal values and *a posteriori* one sigma formal uncertainties. Right ascension and declination are expressed in Earth Mean Equator of 2000 coordinates. Based on the LP47D solution, TCM1 overburned by 1.67% with a pointing error of 0.61°, meeting the execution error requirements for a first burn.[10]

	RA (°)	Dec (°)	ΔV (m/s)
Nominal	279.965	24.395	2.731
Reconstructed	280.618	24.248	2.776
Uncertainties	0.052	0.114	0.004

Table 3. TCM1 estimated values.

The TCM2 reconstruction, identified as V1M25D, was based on a data arc extending 32 days past the burn execution. Roll and yaw wind and unwind turns are not modeled separately since tracking data was not acquired between the start of the yaw wind turn and the end of the roll unwind turn.

An estimate of the sum of TCM2 turns and burn are presented in Table 4 along with the nominal values and *a posteriori* one sigma formal uncertainties. The ΔV vector components are expressed in Earth Mean Equator of 2000 coordinates. Based on the V1M25D solution, TCM2 underburned by 3.5% with a pointing error of 0.51°, again meeting the execution error requirements.

	Δv_x (mm/s)	Δv_y (mm/s)	Δv_z (mm/s)
Nominal	-159.12	45.52	82.87
Reconstructed	-152.73	44.27	81.29
Uncertainties	0.40	0.54	1.44

Table 4. TCM2 estimated values.

TCM3 and TCM4, planned to remove orbit determination errors, were canceled.

TCM Design Support

Orbit determination solutions were generated to support TCM1, TCM2, and TCM3 preliminary and final designs. These solutions and the uncertainties associated with them have been mapped to the Venus B-plane at closest approach and are presented as a series of plots in Figure 8. For reference, the TCM aimpoint, Venus impact radius, and Venus 180 km altitude mapped to the B-plane are also plotted. The 180 km altitude is a conservative estimate of the altitude at which atmospheric drag effects pose a hazard to the spacecraft's health. Most of the shift in orbit solutions between the first and second plots of

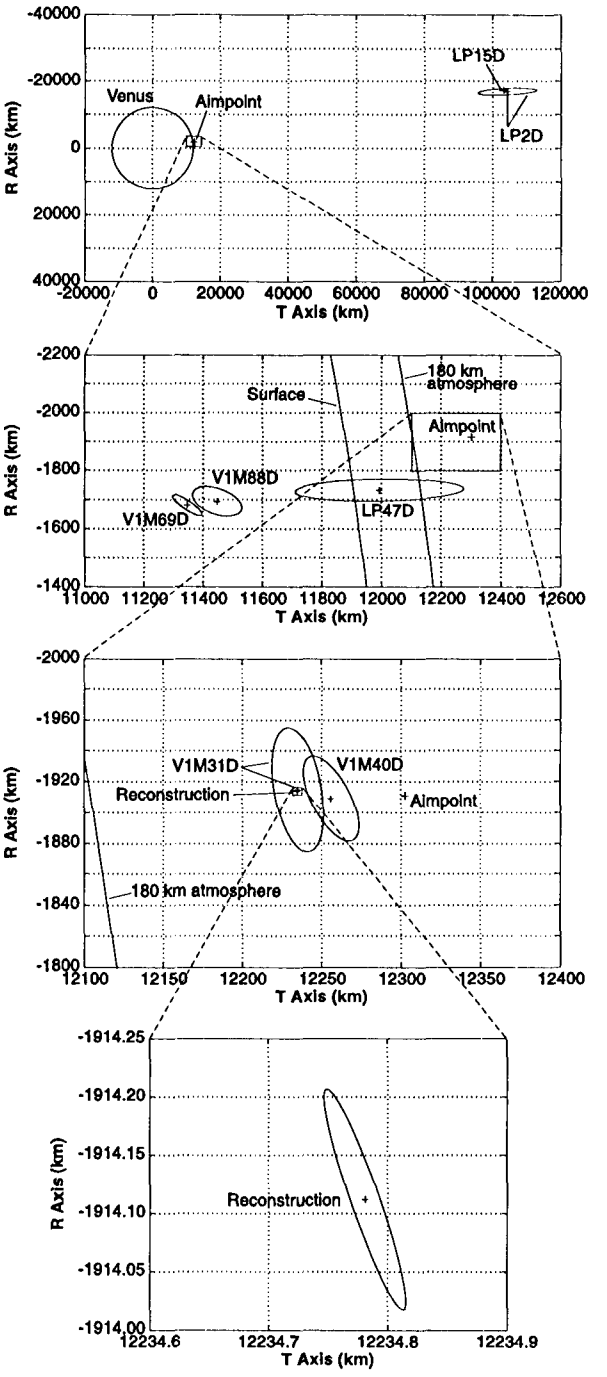

Figure 8. Selected orbit solutions.

Figure 8 can be attributed to TCM1 execution. Similarly, the majority of the shift between the second and third plots can be attributed to TCM2 execution.

The first item to notice in this sequence of plots is that none of the orbit determination error ellipses enclose the aimpoint. This became an expected result upon cancellation of TCM3. An analysis of post-Venus ΔV costs revealed that ΔV costs were not significant if the aimpoint was missed by several tens of kilometers as long as the post-Venus trajectory was modified.[1] The Cassini project opted to forego TCM3 execution in favor of updating the post-Venus trajectory.

Formal statistics are plotted for LP2D, LP15D, and LP47D. After delivery of LP47D, evidence of a modeling error became apparent as solutions began to drift by multiple sigma amounts towards the Venus impact radius. Because the mismodeling was not understood, scale factors were applied to the formal statistics. Scale factors of 5 and 2.2 were applied to V1M88D and V1M69D, respectively. Even so, V1M69D drifted outside of the V1M88D scaled error ellipse. LP47D, the TCM1 reconstruction, has been included in the second plot of Figure 8 to illustrate this mismodeling effect more clearly. A smaller V1M69D scale factor was appropriate because, by this time, the drift was found to be caused by greater than expected Z-thruster firings. The spacecraft torque model was adjusted to compensate. Also, with the realization of extreme sensitivities to mismodeling errors, and noting the low spacecraft declination, Doppler data was de-weighted from 0.2 mm/s to 1.0 mm/s and range data was de-weighted from 5 m to 50 m. Relaxing the tracking data weights served to inflate the formal V1M69D uncertainties.

The third plot from Figure 8 shows the error ellipse growing from V1M40D to V1M31D, a counterintuitive result. The explanation relates to the use of scale factors. V1M40D was scaled by a factor of 3 whereas V1M31D was scaled by a more conservative factor of 4.2. The higher scale factor was the result of maintaining equivalent uncertainties in the Venus miss distance. Conservatism was prudent since these orbit determination uncertainties were used to compute the probability of flying close enough to Venus to damage the spacecraft. Also, unanticipated firing of the Z-thrusters would reduce the Venus miss distance, increasing the probability of damaging the spacecraft.

The final Figure 8 plot shows Cassini's closest approach to Venus based on the reconstructed trajectory. For the flyby reconstruction, tracking data on both the incoming and outgoing trajectory asymptotes are available, enabling a very accurate estimate of the location of closest approach to Venus. The formal one sigma error ellipse uncertainty was scaled by a factor of 13.4 to arrive at a semi-major axis of 100 m. This value was selected after comparing several flyby solutions based on varying data arc lengths, tracking data weights, and *a priori* models and then comparing results.

Estimated values and uncertainties of the linearized time of flight, a measure of orbit uncertainties perpendicular to the B-plane, are presented in Table 5. In this table, linearized time of flight estimates are referenced to the trajectory reconstruction estimate, where a value of zero represents a time of closest approach at 26 April 1998, 13:45:44.3027 ET. A negative value represents an earlier estimated time of closest approach and a positive value represents a later estimated time. Formal one sigma uncertainties have been scaled by the previously specified factors for each solution.

	LTOF (s)	Uncertainty (s)
LP2D	4811.309	465.160
LP15D	4785.428	30.218
LP47D	-9.291	8.291
V1M88D	-39.252	2.365
V1M69D	-41.545	1.536
V1M40D	-1.204	1.986
V1M31D	-0.065	2.432
Reconstruction	0	0.0014

Table 5. Linearized time of flight estimated values and one sigma scaled uncertainties.

Large changes in linearized time of flight estimates subsequent to LP15D are a result of TCM1 execution. Smaller changes subsequent to V1M69D are a result of TCM2 execution.

Orbit Determination Performance

To evaluate orbit determination performance, the error ellipses from Figure 8 are repeated in Figure 9, with the difference that the shifts in orbit solutions attributable to TCMs and spacecraft safing have been eliminated. In other words, the ΔV's from TCM1, TCM2, and spacecraft safing have been modeled in *all* of the solutions. For solutions with data cutoffs preceding these ΔV events, reconstructed ΔV's are modeled. Solutions are plotted relative to the trajectory reconstruction solution instead of the center of Venus.

The first plot in Figure 9 shows that the TCM1 design solutions are consistent with each other and the reconstructed solution. Formal statistics were not scaled for these two solutions.

The second plot in Figure 9 shows that LP47D is more than two sigma from the reconstruction. Statistically, the probability of this shift is less than

	Estimated Value	Formal *a posteriori* sigma
Acceleration Models		
Solar pressure (m^2)	(0.0, 0.0, 18.0)	(0.1, 0.1, 0.3)
RTG radiation (km/s^2)	(-0.9, -0.1, 1.0)x10^{-12}	(0.1, 0.1, 0.4)x10^{-12}
Outgassing (km/s^2) time constant (days)	(-0.1, -4.3, -4.3)x10^{-12} 28.6	(0.2, 2.4, 0.4)x10^{-12} 4.0
15 January 1998 RWA maintenance (km/s^2)† duration = 36 hrs, time constant = 5 days	-2.6x10^{-12}	0.5x10^{-12}
Slow roll end (km/s^2)† duration = 39 hrs, time constant = 5 days	-0.9x10^{-12}	0.1x10^{-12}
Post TCM2 (km/s^2)† duration = 59 hrs, time constant = 5 days	-1.7x10^{-12}	0.2x10^{-12}
Spacecraft safing (km/s^2)† duration = 10 hrs, time constant = 5 days	-9.4x10^{-12}	2.5x10^{-12}
Gravity gradient - incoming asymptote (km/s^2)† duration = 2 hrs, time constant = 45 minutes	-42.0x10^{-12}	11.4x10^{-12}
Gravity gradient - outgoing asymptote (km/s^2)† duration = 2 hrs, time constant = 4 hours	-788x10^{-12}	205x10^{-12}
1 May 1998 RWA maintenance (km/s^2)† duration = 36 hrs, time constant = 5 days	-1.7x10^{-12}	0.8x10^{-12}
ΔV Models (mm/s)		
Center_Sun mode - 15 October 97 15:46	(-0.6, -0.2, -4.4)	(0.4, 0.5, 0.5)
Center_Sun mode - 16 October 97 01:18	(-0.1, 0.6, -3.7)	(0.5, 0.5, 0.6)
Center_Sun mode - 16 October 97 07:14	(0.7, -0.3, -3.8)	(0.4, 0.5, 0.6)
Center_Sun mode - 16 October 97 14:36	(0.7, -0.5, -4.9)	(0.4, 0.5, 0.6)
Center_Sun mode - 16 October 97 22:07	(0.0, 0.0, -4.1)	(0.4, 0.5, 0.6)
Center_Sun mode - 17 October 97 02:39	(-0.6, 0.1, -3.8)	(0.4, 0.5, 0.5)
Center_Sun mode - 17 October 97 09:00	(-1.0, 0.2, -3.7)	(0.4, 0.5, 0.5)
Attitude control reset	(-0.6, 0.2, 0.8)	(0.3, 2.6, 0.6)
Vent/prime main engines	(0.7, 0.2, -3.9)	(0.5, 0.5, 1.1)
Tighten attitude control deadbands	(-0.2, 0.0, -1.5)	(0.4, 0.5, 1.1)
TCM1 roll wind turn*	(-0.1, 0.0, 0.0)	(0.3, 0.5, 0.5)
TCM1 yaw wind turn*	(-0.9, -9.8, 0.2)	(0.9, 1.8, 2.0)
TCM1 (RA, Dec, ΔV estimated)*	(280.7°, 24.3°, 2.775 m/s)	(0.04°, 0.09°, 0.003 m/s)
TCM1 yaw unwind turn*	(-3.0, -8.7, 0.3)	(0.9, 1.8, 2.0)
TCM1 roll unwind turn*	(-0.2, 0.1, 0.0)	(0.2, 0.5, 0.5)
RWA Maintenance - 15 January 98	(-0.1, 0.1, -1.2)	(0.1, 1.0, 0.1)
TCM2*	(-153.3, 43.7, 81.5)	(0.2, 0.5, 1.3)
RCS firing, undetermined cause - 17 March 98†	-0.1	0.1
RCS firing, undetermined cause - 20 March 98†	-0.1	0.1
RCS firing, undetermined cause - 21 March 98†	-0.1	0.1
Spacecraft safing	(-0.1, 0.1, -4.6)	(0.04, 0.8, 0.2)
RWA maintenance - 1 May 98	(0.1, 0.0, -1.3)	(0.1, 0.5, 0.2)

* Earth Mean Equator of 2000 coordinates. † Only spacecraft-fixed Z-component estimated.

Table 6. Estimated values and uncertainties based on trajectory reconstruction.

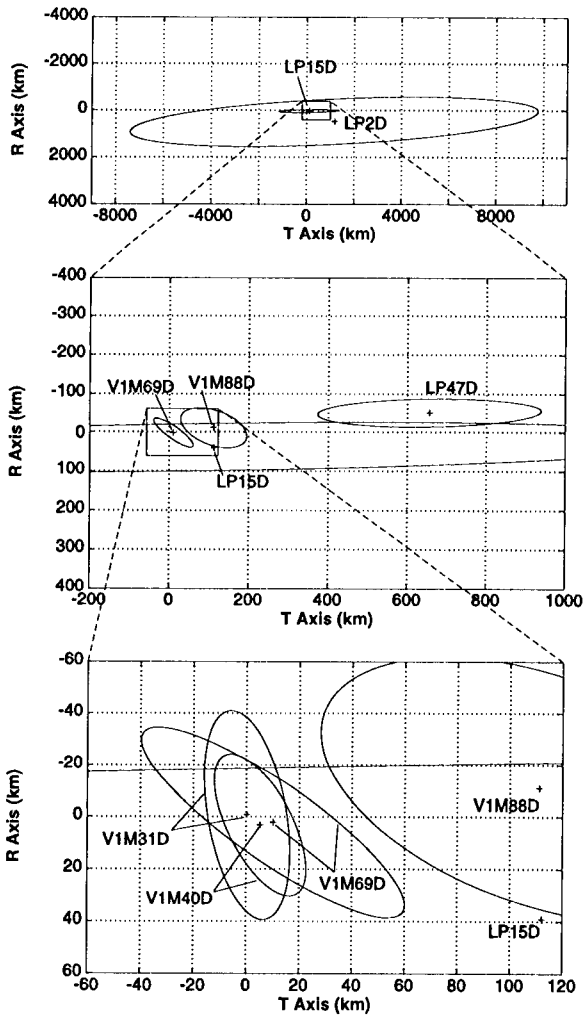

Figure 9. Selected orbit solutions with all significant ΔV events modeled.

5%, indicating a mismodeling error. Mismodeling of Z-thruster firings, as described previously, accounted for most of this shift. V1M88D and V1M69D are consistent with the reconstructed solution. Formal statistics from LP47D were not scaled. Formal statistics from V1M88D and V1M69D were scaled by factors of 5 and 2.2 respectively, reflecting the confidence in modeling.

The third plot of Figure 9 shows that the TCM3 design solutions and V1M69D are consistent with the reconstructed solution. Scale factors of 3 and 4.2 have been applied to V1M40D and V1M31D respectively. In hindsight, the grouping of the three plotted solutions suggests that the scale factors are very conservative. In an operations sense, however, the penalty for optimistic estimates was unacceptable when flying so close to Venus.

Reconstruction of Venus Flyby

The Venus flyby trajectory can be reconstructed very accurately when tracking data is acquired on both the incoming and outgoing trajectory asymptotes. The data arc for the trajectory reconstruction ends 17 days after the Venus flyby. The solution is based on two-way Doppler weighted at 0.2 mm/s, range weighted at 50 m, and the *a priori* models discussed previously. Two-way Doppler and range residual plots are included as Figures 10 and 11. Plotted numbers refer to the tracking stations that made the measurements.

Estimated values and formal one sigma *a posteriori* uncertainties are listed in Table 6. Correlations exist between most of these parameters but are not listed. Acceleration and ΔV estimates are listed in spacecraft fixed coordinates unless stated otherwise. Exponential acceleration values are initial values, prior to decay. Solar pressure accelerations are listed as 'effective areas', described previously.

Several values listed in Table 6 deserve special attention. The Z-component of the solar pressure model represents a four sigma change from the nominal value of 20.9 m^2. The Z-component of the RTG re-radiation model is positive when, in fact, it should be negative. These values suggest that there is still some mismodeling present in the long term acceleration models. These inconsistencies are currently being investigated. In contrast, short term acceleration models all have the expected polarity.

Gravity gradient accelerations appear quite large, especially on the outgoing asymptote. However, these accelerations decay quickly and act over a short time interval. They represent an effective ΔV of only a few millimeters per second.

TCM1 and TCM2 estimated values from Table 6 differ from the TCM reconstructions described earlier, but are still consistent with the one sigma formal uncertainties given in Tables 3 and 4. Differences are caused by longer data arc lengths and orbit determination filter initializations.

Venus and Earth planet corrections in radial, downtrack, and out-of-plane coordinates are listed in Table 7. These corrections are all smaller than the one sigma *a priori* uncertainties of (0.008, 2.23, 3.11) km for Earth and (0.18, 2.05, 3.41) km for Venus.

	Radial (km)	Downtrack (km)	Crosstrack (km)
Earth	0.	1.88	-2.94
Venus	-0.08	1.23	1.92

Table 7. Corrections to Earth and Venus ephemerides at time of Venus closest approach.

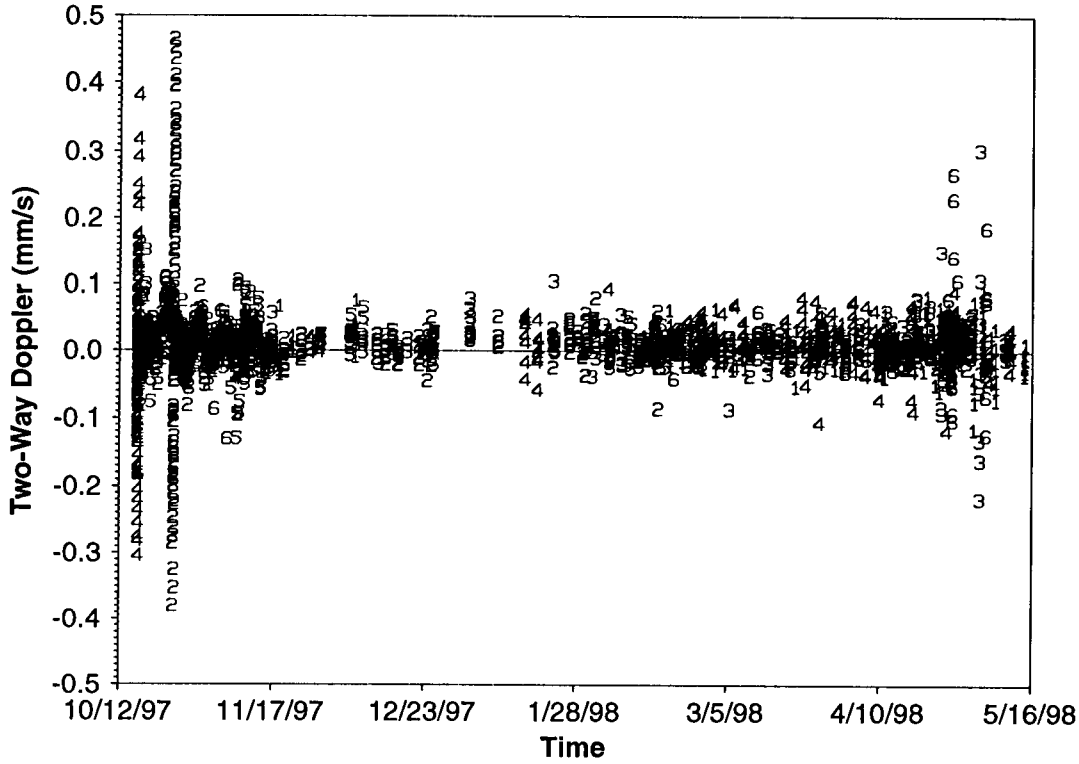

Figure 10. Two-way Doppler residuals based on trajectory reconstruction.

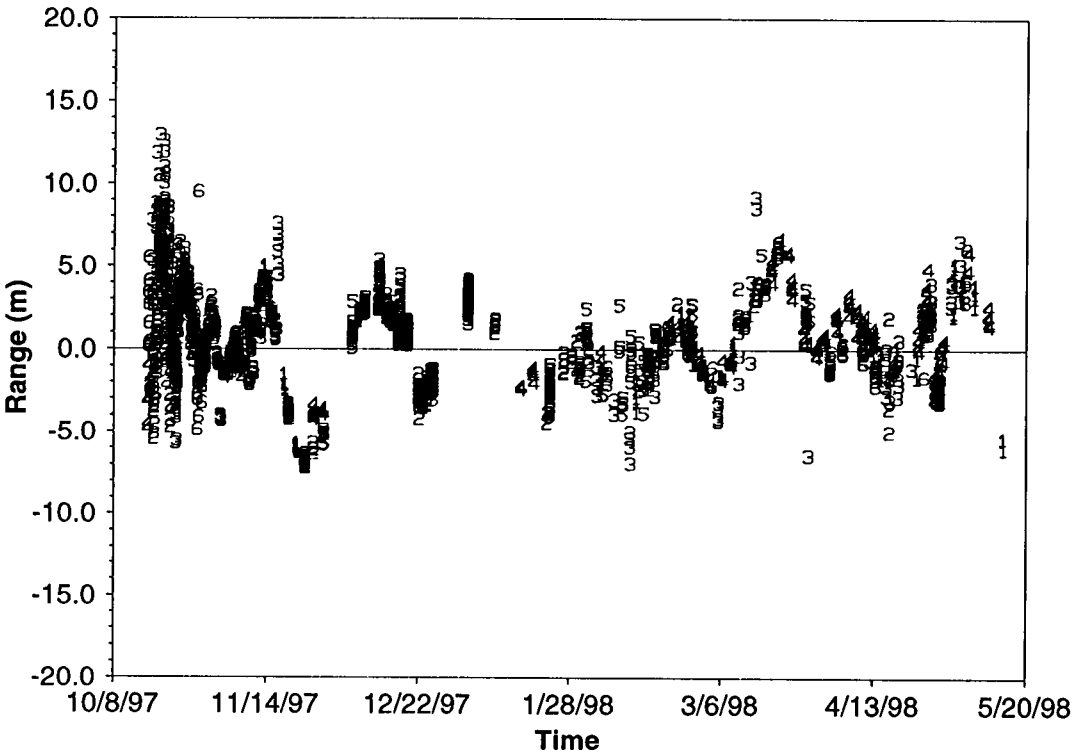

Figure 11. Range residuals based on trajectory reconstruction.

Concluding Remarks

The first Cassini flyby of Venus was extremely successful. Only two of the four planned trajectory correction maneuvers were needed. Navigation predictions of Cassini's Venus relative periapsis, based on orbit solutions with data cutoffs more than one month prior to the flyby, were accurate to within one kilometer. The time of closest approach was predicted to within 35 milliseconds.

Much experience has been gained during this first leg of the interplanetary mission. This experience will be invaluable in navigating Cassini to the next Venus flyby on 24 June 1999 and the ensuing Earth flyby on 18 August 1999.

Appendix

The B-plane, shown in Figure 12, is a plane passing through the center of the target body and perpendicular to the incoming asymptote of the hyperbolic flyby trajectory. Coordinates in the plane are given in the **R** and **T** directions, with T being parallel to the Earth Mean Orbital plane of 2000. The angle θ determines the rotation of the semi-major axis of the error ellipse in the B-plane relative to the T-axis and is measured positive right-handed about S.

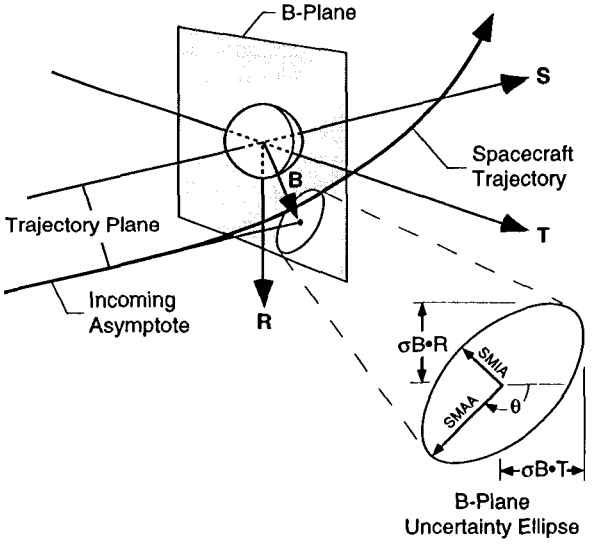

Figure 12. The B-plane coordinate system.

Acknowledgments

The research described in this paper was performed at the Jet Propulsion Laboratory, California Institute of Technology, under contract with the National Aeronautics and Space Administration.

References

1. Goodson, T. D., Gray, D. L., Hahn, Y., Peralta, F., "Cassini Maneuver Experience: Launch and Early Cruise", AIAA Guidance, Navigation, and Control Conference, Boston, Massachusetts, 10 - 12 August 1998.

2. Hamilton, T. W., and Melbourne, W. G., "Information Content of a Single Pass of Doppler Data from a Distant Spacecraft", JPL Space Programs Summary, No. 37-39, Vol. III, March - April 1966, pp. 18-23.

3. Thurman, S. W., "Comparison of Earth-Based Radio Metric Data Strategies for Deep Space Navigation", AIAA/AAS Astrodynamics Conference, Portland, Oregon, 20 - 22 August 1990.

4. "Cassini Navigation Plan", Cassini Project Document 699-101 (internal document), Jet Propulsion Laboratory, Pasadena, California, 29 May 1996.

5. "Control Analysis Book", Cassini Project Document 699-410 (internal document), Chapter 4.2, Jet Propulsion Laboratory, Pasadena, California, 2 February 1996.

6. Clough, D., "Trajectory Correction Maneuver 2 (TCM2) Final Report Summary", JPL Interoffice Memorandum 313N-98-023 (internal document), Jet Propulsion Laboratory, Pasadena, California, 18 May 1998.

7. Lisman, S., "Cassini Non-Gravitational Force and Torque Estimates, Final Guidance Analysis Book Documentation", JPL Interoffice Memorandum 3456-94-004 (internal document), Jet Propulsion Laboratory, Pasadena, California, 8 August 1994.

8. Standish, E. M., personal communication, 18 July 1997.

9. Folkner, W. M., "Current DSN station locations", JPL Interoffice Memorandum 335.1-95-027 (internal document), Jet Propulsion Laboratory, Pasadena, California, 16 October 1995.

10. "Accuracy Requirement and System Capabilities, Rev. D", Cassini Project Document 699-205-3-170 (internal document), Jet Propulsion Laboratory, Pasadena, California, 7 November 1997.